

High-resolution extracellular stimulation of dispersed hippocampal culture with high-density CMOS multielectrode array based on non-Faradaic electrodes

This article has been downloaded from IOPscience. Please scroll down to see the full text article.

2011 J. Neural Eng. 8 044003

(<http://iopscience.iop.org/1741-2552/8/4/044003>)

View [the table of contents for this issue](#), or go to the [journal homepage](#) for more

Download details:

IP Address: 144.214.96.72

The article was downloaded on 26/10/2011 at 04:36

Please note that [terms and conditions apply](#).

COMMUNICATION

High-resolution extracellular stimulation of dispersed hippocampal culture with high-density CMOS multielectrode array based on non-Faradaic electrodes

N Lei¹, S Ramakrishnan¹, P Shi², J S Orcutt³, R Yuste⁴, L C Kam² and K L Shepard¹

¹ Bioelectronic Systems Lab, Department of Electrical Engineering, Columbia University, 500 West 120th Street 1300, New York, NY, USA

² Microscale Biocomplexity Laboratory, Department of Biomedical Engineering, Columbia University, 351 Engineering Terrace, New York, NY, USA

³ Department of Electrical Engineering and Computer Science, Massachusetts Institute of Technology, 77 Massachusetts Avenue, Cambridge, MA, USA

⁴ Department of Biological Sciences, Columbia University, 901 NWC Building, New York, NY, USA

E-mail: leina@ee.columbia.edu

Received 3 March 2011

Accepted for publication 17 June 2011

Published 4 July 2011

Online at stacks.iop.org/JNE/8/044003

Abstract

We introduce a method to electrically stimulate individual neurons at single-cell resolution in arbitrary spatiotemporal patterns with precise control over stimulation thresholds. By exploiting a custom microelectronic chip, up to 65 000 non-Faradaic electrodes can be uniquely addressed with electrode density exceeding 6500 electrodes mm⁻². We demonstrate extracellular stimulation of dispersed primary hippocampal neuronal cultures using the chip at single-cell resolution.

(Some figures in this article are in colour only in the electronic version)

1. Introduction

Large neural circuits composed of multiple cells connected in complex networks exhibit specific functional behaviors. Systematic neural stimulation at one or multiple sites within the network is essential in understanding the functioning of these circuits. Very recently, techniques for photostimulation based on uncaging of MNI-glutamate (Nikolenko *et al* 2007) and transgenic rhodopsin channels (Wang *et al* 2007, Aravanis *et al* 2007) have been developed and applied to both dispersed cultures and brain slices. When combined with whole-cell recording on a neuron, these techniques can detect monosynaptically connected cells and allow network connectivity to be determined by mapping presynaptic

inputs (Nikolenko *et al* 2007, Matsuzaki *et al* 2008). However, photostimulation using directed beam or spatial light modulators (Lutz *et al* 2008) allows only few-cell-per-trial activation, significantly reducing stimulation throughput and limiting the efficacy of this approach.

Microelectrode arrays (MEAs) are an alternative stimulation modality with microelectrodes fabricated on a planar substrate and aligned into an array at a fixed pitch. Typical planar passive MEAs have 128 electrodes at a density of 60 electrodes mm⁻² with 20–70 μm square size at a 100–450 μm pitch (Hai *et al* 2010, Thiebaud *et al* 1997, Potter and DeMarse 2001). Electrophysiological readout from passive MEA is limited by the number of external measurement channels and the required wired connections to them from

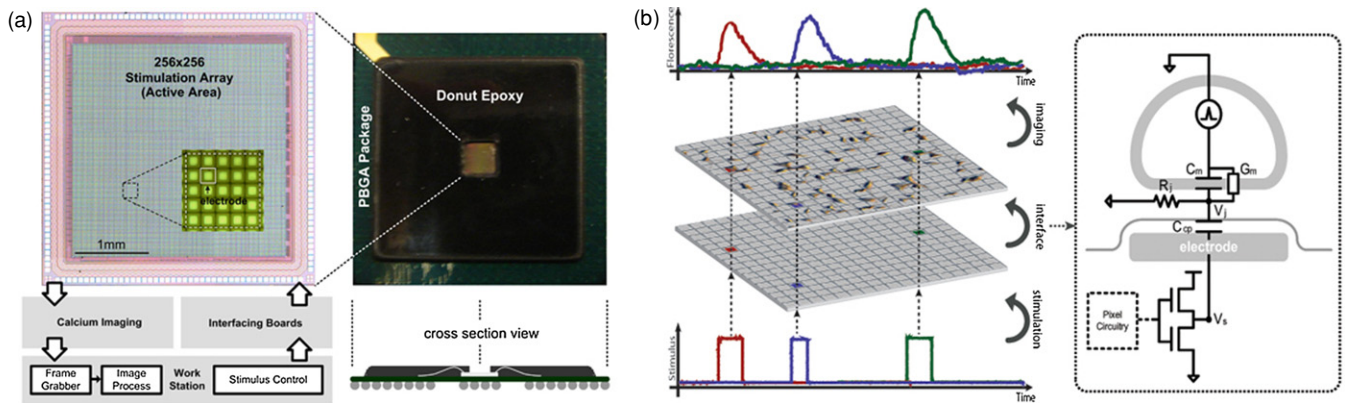


Figure 1. Configuration of the high-resolution MEA microsystem. (a) High-resolution stimulation microsystem platform composed of integrated CMOS MEA and optical recording microscopy. Chip package using ball grid array is shown. (b) Working principle of the microsystem. Expansion illustrates a lumped model of the neuron–capacitor–silicon interface.

the substrate. Low electrode density is necessary to cover large recording areas, resulting in an average inter-electrode spacing of $150\ \mu\text{m}$, which is far larger than the typical inter-cell spacing of $10\text{--}15\ \mu\text{m}$.

Very recently, complementary metal–oxide–semiconductor (CMOS) technology has been used to create a new generation of active MEAs (Eversmann *et al* 2003, Heer *et al* 2007, Lambacher *et al* 2004, Berdondini *et al* 2005, 2009). With stimulation or record electronics integrated directly onto the same substrate with the electrode array, active MEAs can achieve significantly higher electrode densities than passive structures, typically several thousand electrodes per mm^2 (Frey *et al* 2009, Hutzler *et al* 2006). Prior work on active MEAs has relied mostly on traditional Faradaic electrodes and integrated electronics for extracellular recording.

In this paper, we instead focus on stimulation, relying on optical techniques for record, and employ non-Faradaic electrode interfaces. A 256×256 electrode array within a $9\ \text{mm}^2$ area delivers 65 000 parallel and simultaneous stimulation channels with a $1.3\ \mu\text{s}$ refresh rate. The stimuli from any two electrodes in the array can be synchronized and aligned within $45.7\ \text{ps}$ with $125\ \text{ns}$ pulse resolution. Electrodes on our active MEA are isotropically coated with a high- κ metal oxide, hafnium oxide (HfO_2 , figure 1(b)), and stimulation occurs entirely through displacement currents. The use of capacitively coupled electrodes blocks Faradaic reactions at the interface, thereby preventing electrochemical corrosion of electrodes, cell damage, water electrolysis and changes in chemical environment near the cell, such as pH deviation (Brummer and Turner 1977, Brummer *et al* 1983, Hambrecht 1979). Charge injection, however, is typically $15\ \mu\text{C cm}^{-2}$, lower than traditional Faradaic platinum or platinum–iridium electrodes at $50\text{--}300\ \mu\text{C cm}^{-2}$ (Rose and Robblee 1990, Cogan *et al* 2005, Stensaas and Stensaas 1978, Rose *et al* 1985). While there is often concern that capacitive electrodes may lead to insufficient current for stimulation (Cogan 2008), we show the ability in dispersed cultures to control stimulation of individual cells through these electrode interfaces.

2. Materials and methods

2.1. High-resolution CMOS MEA system platform

The CMOS MEA designed here, and described elsewhere (Lei *et al* 2008), allows the activation of arbitrary combinations of electrodes within the array with unique stimulation pulse trains. The $4\ \text{mm} \times 4\ \text{mm}$ MEA consists of a 256×256 electrode array (figure 1(a)). Each square electrode has an edge length of $11.4\ \mu\text{m}$ and a pitch of $12.2\ \mu\text{m}$, giving rise to a total active stimulation area of $3 \times 3\ \text{mm}^2$ with an electrode density of $6724\ \text{mm}^{-2}$. The electrodes are realized using the top aluminum metal layer in the CMOS technology, augmented by post-processing steps outlined in section 2.2 to make capacitive electrodes. A per-electrode integrated pulse generator independently configures unique voltage pulse stimuli at each electrode. A programmable stimulus amplitude applies to all MEA electrodes. Pixel circuitry is constructed underneath each electrode, occupying an area of $12.2\ \mu\text{m}^2$.

A customized six-layer printed circuit board sockets the packaged MEA (figure 1(a)). Two external data acquisition cards (NIDAQ, National Instruments) provide stimulation bit patterns to the MEA, which encode electrode coordinates of the pixels to be activated, the pulse duration, duty cycle and the number of pulses. A stimulus train consisting of 14 pulses each with $200\ \mu\text{s}$ duration at $10\ \text{ms}$ period is applied to the MEA electrode throughout the experiments. The experiments combine electrical stimulation from the MEA electrodes with optical recording, utilizing Ca^{2+} sensitive dyes to observe intracellular calcium concentration change as an indirect measure of action potential (figure 1(b)). An external trigger sent to both the recording camera and the NIDAQ acquisition cards allows synchronization.

Figure 1(b) shows the lumped circuit model of the interface between a soma and a capacitive MEA electrode. Biphasic displacement currents from the electrode produce a local voltage gradient V_j through the cleft resistance R_j . Local depolarization of the cell membrane occurs with a changing V_j relative to the bath voltage fixed by an external reference electrode (Schoen and Fromherz 2007).

2.2. Extended microfabrication

The MEA is fabricated in a commercial CMOS foundry (Taiwan Semiconductor Manufacturing Company) with a minimum transistor length of 0.25 μm and operating at a nominal voltage of 2.5 V. This commercial CMOS foundry process leaves a passivation layer of 0.7 μm of Si_3N_4 and 1 μm of SiO_2 on top of the electrodes. To expose the electrodes, this layer is etched (as a post process) using dry-etch with a composite gas of C_4F_8 and O_2 . A photoresist mask restricts this etch to the array area of the chip. After this etch, the metal electrodes protrude from the surface by approximately 1 μm . A low-temperature atomic-layer-deposition process is then used to directly deposit an isotropic 20 nm HfO_2 layer onto these electrodes.

2.3. Hippocampal cell culture

Prior to cell culture, chips are sterilized in Linbro 7X detergent at 100 $^\circ\text{C}$ for 45 min, then rinsed extensively with deionized water, which is followed by dehydration at 120 $^\circ\text{C}$ for 1 h. A 10 mm tall polypropylene well is attached to the chip and sealed with PDMS to form a 15 mm diameter culture well. Each chip is coated with 100 $\mu\text{g ml}^{-1}$ poly-L-lysine (Sigma-Aldrich) and 10 $\mu\text{g ml}^{-1}$ laminin (Invitrogen) overnight at room temperature. Both solutions are diluted in phosphate buffered saline (pH 7.4, Invitrogen).

Hippocampal neuronal cultures are prepared following the method previously described (Banker and Goslin 1998). Briefly, neurons are prepared by enzymatic (Papain, Sigma) and mechanical dissociation of hippocampi from E18 Sprague–Dawley rats. Cells are plated at a density of 5000 cell cm^{-2} onto the array in Dulbecco's modified eagle medium (DMEM, Invitrogen) containing 10% fetal bovine serum. Chips with plated cells are then incubated for 2 h with 5% CO_2 and 95% humidity at 37 $^\circ\text{C}$ to allow cell attachment. After incubation, the medium is replaced with serum-free neurobasal containing B27 supplements, 0.5 mM L-glutamate and 100 unit ml^{-1} penicillin and streptomycin. For each culture, half of the medium is changed every three days before usage, and are incubated for 14 days *in vitro* (DIV) prior to experimentation.

2.4. Fluorescence imaging with calcium signaling

The chip containing neural cultures is imaged and recorded using the high-affinity indicator Fluo-4-AM ($\kappa_D = 350$ nM, Invitrogen). Calcium indicator loading is carried out using established protocols. Briefly, cells are loaded with 1 μM Fluo-4-AM dye in filtered phenol-red-free DMEM buffered with 20 mM HEPES (pH 7.3) in an incubator at 37 $^\circ\text{C}$ for 30 min. Extra dye is washed off after incubation, and experiments are performed with cell culture immersed in a warmed DMEM–HEPES solution.

Changes in intracellular calcium concentration are captured using a cooled-CCD camera (Orca ER, Hamamatsu) mounted on an upright fluorescence microscope (BX50WI, Olympus) with 490 nm excitation and 520 nm emission filters.

Time-lapse fluorescence images are taken at 10 Hz (one-by-one binning) and 25 Hz (four-by-four binning), using either 10 \times /NA-0.3 air objective or 20 \times /NA-0.5 water immersion objective (UMPlan FL, Olympus). Imaging is performed in a dark environment with images collected using IPLab (BioVision Technologies).

Acquired images are analyzed by fluorescence change over time using

$$\Delta F/F_0 = \frac{(F_i - B_i) - (F_0 - B_0)}{(F_0 - B_0)},$$

where F_0 and F_i are fluorescence at the beginning of the experiment and at any given time point, respectively, and B_0 and B_i are the associated fluorescence background intensities. $\Delta F/F_0$ is a background-corrected pixel-wise subtraction of each frame from the first frame with the difference normalized to the fluorescence intensity of the first frame. Analysis is done by calculating $\Delta F/F_0$ from the original movie, and adjusting the look-up table so that pixels associated with increasing calcium fluorescence appear white versus a dark background. Relative $\Delta F/F_0$ is generated using a preprogrammed Java plug-in in ImageJ imaging software (NIH).

2.5. Immunohistochemistry

Following optical imaging of hippocampal neurons on chip, the cells are fixed using 4% paraformaldehyde in PBS (pH 7.4) for 15 min at room temperature. Cells are rinsed with 1% bovine serum albumin (BSA) solution (in PBS) and then incubated in 0.1% Triton-X100 solution for 1 h. The neurons are then washed with 1% BSA solution followed by anti-beta tubulin (a neuronal marker) and anti-synapsin (a synaptic marker) incubation for 30 min at room temperature. Primary antibodies are rinsed off with PBS. FITC-anti mouse and rhodamine-anti rat are used as secondary antibodies at 1:1000 dilution. After 30 min incubation, they are washed off and the labeled neural cultures are imaged using 488 and 615 nm filters on the upright microscope.

3. Results

3.1. Fluorescence calibration

Prior to characterization of MEA stimulation, we calibrate fluorescent recording of calcium transients with synchronized electrophysiological recording of spontaneous activity. Neural activities are recorded with cell-attached loose-patch using 3–6 $\text{M}\Omega$ pipettes filled with 20 mM HEPES–DMEM. The microelectrodes are pulled from 1.5 mm outer diameter and 0.86 mm inner diameter borosilicate glass tubes. The glass microelectrode is slowly lowered into solution and the cell is approached, until a 10–30 $\text{M}\Omega$ seal is achieved. Action currents from these cells are recorded using a patch clamp amplifier (EPC10, HEKA Elektronik), at 20 mV pA^{-1} gain with signals filtered (Bessel) and sampled at 10 kHz.

Cells from dissociated hippocampal cultures are grown on the array (figure 2(a)). Action potential spikes 4 dB above the noise average are considered to be action currents. Calcium transients are imaged at 25 Hz for 30 s intervals.

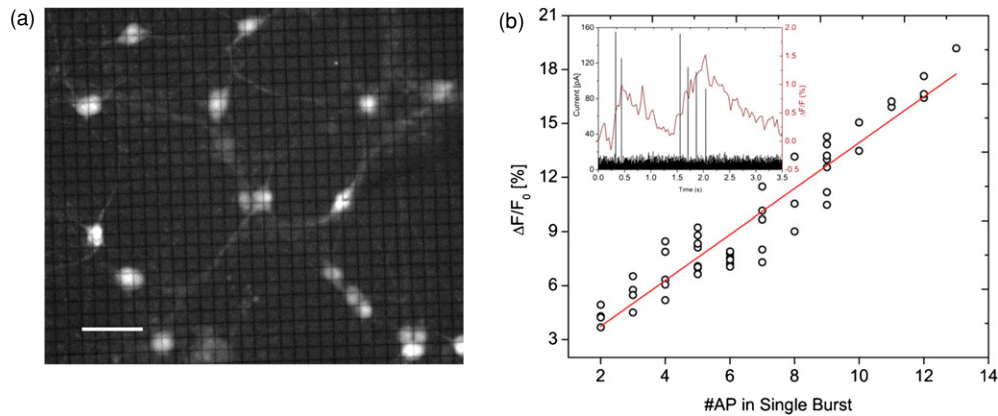


Figure 2. (a) Fluo-4 fluorescence of disperse culture growth on MEA surface. (b) Calibration curve correlating the number of action potential in a single burst with percent change in calcium fluorescence. The inset shows the raw trace of loose-patch electrophysiology with simultaneous recording of calcium signals. Results are taken over six cells. Scale bar equals $50 \mu\text{m}$.

Peak $\Delta F/F_0$ is used in the calibration. We compare action potential (AP) burst (firing frequency > 6.5 Hz) captured in the electrophysiological recordings with discrete Ca^{2+} signals summed consecutively in the soma (figure 2(b)). The measured fluorescence response to AP bursts shows distinct change in the case of more than two APs, with the occurrence of fluorescent peaks time-locked to the last AP within the corresponding bursts. Detecting a single AP response is limited by a signal-to-noise ratio of approximately 1 in this case. The $\Delta F/F_0$ versus AP train shows a 1.27% fluorescence change per AP. This calibration curve is used to deduce AP numbers in future experiments.

3.2. Stimulus characterization

To characterize electrode stimulation current in solution in the absence of a cell, we measure the transient artifact in response to varying amplitudes applied to a single target electrode. An AgCl external electrode positioned above the electrode is used to measure this time transient in the absence of cells in a DMEM-HEPES solution. Because of the capacitive coupling of the electrode to the solution, the voltage pulse applied to the electrode produces a biphasic current stimulation. Figure 3 shows the measured time transient of a biphasic current stimulus in response to pulses applied to a single target electrode at different amplitudes. Each electrode has a capacitance of 0.9 pF , delivering 20 pC of charge at 1.6 V . The peak biphasic current is approximately 85 pA V^{-1} of amplitude for the rising edge of the pulse and 35 pA V^{-1} of amplitude for the trailing edge. The junction potential change created by the biphasic current with an attached cell can be expected to be substantially higher than without the cell because of the higher resistance in the cleft between the cell and the electrode.

3.3. Single-cell stimulation threshold

We next explore the ability to stimulate individual cells controllably from the on-chip electrodes. Stimulation pulse trains of varying amplitudes are delivered to cells whose

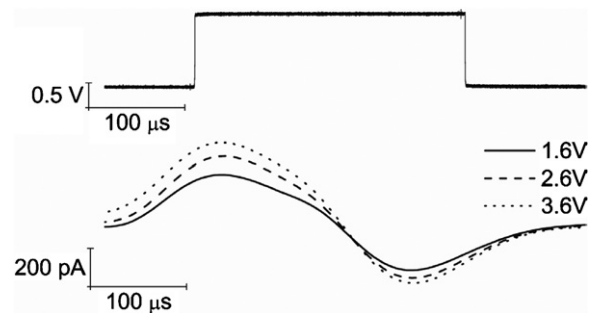


Figure 3. Square voltage pulse stimulus produced by individual MEA electrodes (top) and the triggered stimulus artifact in a $1 \times$ DMEM-HEPES solution (bottom).

somata are in direct contact with the target electrodes. Fluorescence signals from cells are recorded simultaneously at 10 Hz . We image the spontaneous activity of the target neurons immediately following each stimulation experiment to confirm that the activity observed is a result of the stimulation applied. Figure 4 shows stimulation-induced peak $\Delta F/F_0$ values as a function of stimulation amplitudes from four neurons on three arrays. We define the activation threshold as the minimum stimulation amplitude needed to reliably elicit 1.27% fluorescence change per AP over unstimulated spontaneous baseline activity. At this percentage level, an extrapolated activation threshold is approximately 1.5 V .

3.4. Artifact stimulation due to electrolyte coupling

We also study the precision with which we can stimulate individual cells. For good spatial resolution, stimulation should activate only the target neuron in contact with the MEA electrode. Free electrodes, with no neural growth on them, are identified at progressive distances of one to nine electrodes from a target cell. At each location, the activation threshold of the target cell is determined by sequentially stepping through stimulation amplitudes and inducing fluorescence change over

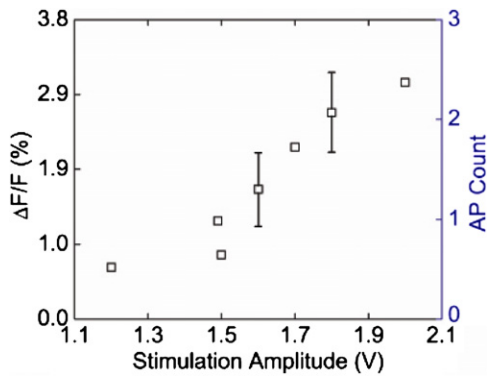


Figure 4. Somatic peak $\Delta F/F_0$ in response to stimulus at various amplitudes. AP—action potential.

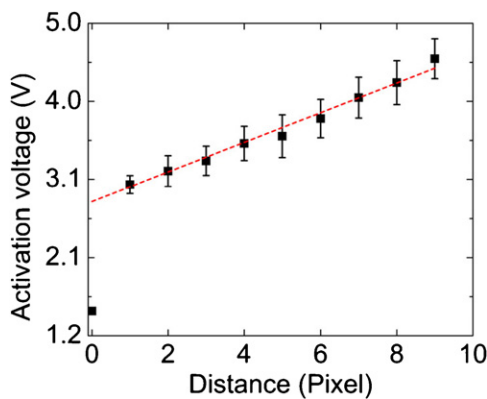


Figure 5. Effect of electrode stimulation at varying distances from the target cell on neural activation.

the baseline in the target cell for 1.27% $\Delta F/F_0$. Figure 5 shows the activation threshold as a function of electrode distance with a linear dependence of approximately 18 mV μm^{-1} for non-contacting electrodes. The contacting electrode (zero distance in figure 5) requires a substantially lower stimulation voltage

due to the fact that displacement currents in this case result in a higher effective extracellular stimulation voltage due to higher seal resistance of the cell–electrode cleft region (Schoen and Fromherz 2007). It is this nonlinearity that allows for targeted single-cell stimulation. Error bars are determined from four different cells across three arrays.

3.5. Cellular level selective stimulation

To demonstrate targeted cell stimulation, we stimulated individual neurons of the cultured networks shown in figure 6, consisting of five cells. Each cell is sequentially stimulated with the associated target electrodes below the cell. In each trial, we analyze the evoked AP response in the stimulated cell and neighboring cells. In five stimulation trials, one of the cells did not respond to stimulation. The remaining four exhibit significant activation upon targeted stimulation, while non-stimulated cells show no activity. Stimulated cells have an average relative fluorescence change of $4.24\% \pm 1.22$, corresponding to three APs, while non-stimulated ones yield $0.23\% \pm 0.03$ ($n = 5$ neurons; $p = 0.048$, two-tailed). Activity did not spread synaptically from the target neurons.

4. Conclusion

In this paper, we present a MEA with 65 000 electrodes on an active CMOS chip, capable of providing high-density high-resolution stimulation patterns using non-Faradaic electrode interfaces. We demonstrate the ability to use these MEA electrodes to accurately and precisely stimulate neuron cultures at single-cell resolution. Since functional connections between cells can be reconstructed through stimulation at one or multiple pre-synaptic neurons (Holmgren *et al* 2003, Thomson *et al* 2002), the high density of electrodes, the parallel stimulation capabilities and the selectivity for stimulation characteristics of this MEA make it a useful tool for reverse-engineering connectivity in neural circuits.

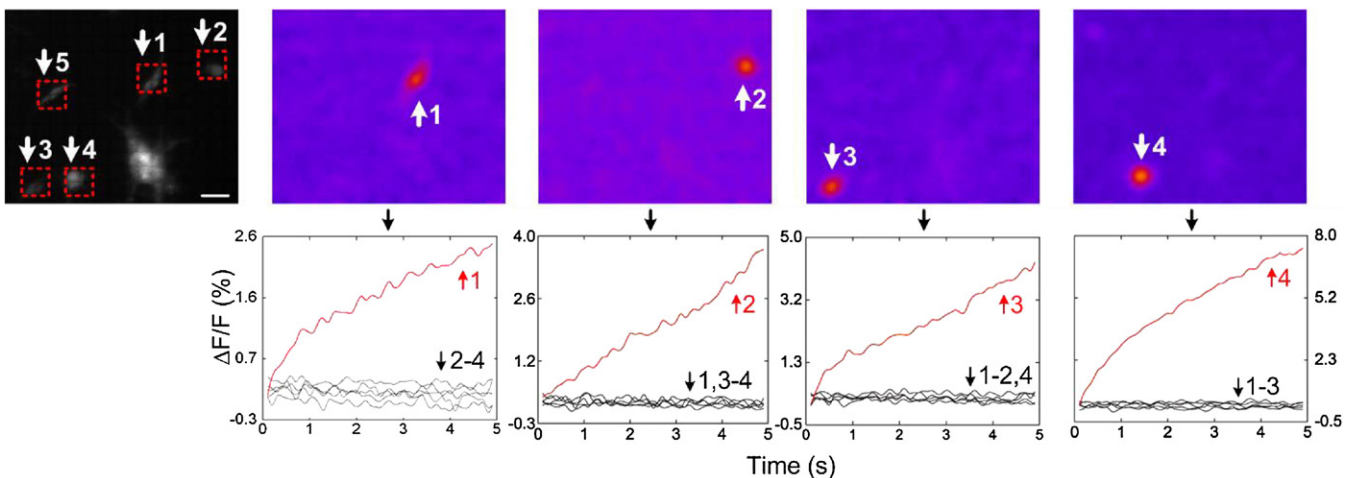


Figure 6. Fluo-4 fluorescence (top left) and time averaged $\Delta F/F_0$ intensity evoked by extracellular stimulation at 2.5, 2.7, 2.7 and 2.2 V for cells 1 to 4, respectively. The arrows mark five individual neurons. The bottom traces show temporal responses. Scale bar equals 20 μm .

Acknowledgements

This work is supported in part by the New York State Foundation for Science, Technology, and Innovation (NYSTAR) and the Gatsby Initiative in Brain Circuitry.

References

- Aravanis A M, Wang L P, Zhang F, Meltzer L A, Mogri M Z, Schneider M B and Deisseroth K 2007 An optical neural interface: *in vivo* control of rodent motor cortex with integrated fiberoptic and optogenetic technology *J. Neural Eng.* **4** S143–56
- Banker G and Goslin K 1998 *Culturing Nerve Cells* (Cambridge, MA: MIT Press)
- Berdondini L, Imfeld K, Maccione A, Tedesco M, Neukom S, Koudelka-Hep M and Martinoia S 2009 Active pixel sensor array for high spatio-temporal resolution electrophysiological recordings from single cell to large scale neuronal networks *Lab Chip* **9** 2644–51
- Berdondini L, van der Wal P D, Guenat O, de Rooij N F, Koudelka-Hep M, Seitz P, Kaufmann R, Metzler P, Blanc N and Rohr S 2005 High-density electrode array for imaging *in vitro* electrophysiological activity *Biosens. Bioelectron.* **21** 167–74
- Brummer S B, Robblee L S and Hambrecht F T 1983 Criteria for selecting electrodes for electrical-stimulation—theoretical and practical considerations *Ann. New York Acad. Sci.* **405** 159–71
- Brummer S B and Turner M J 1977 Electrochemical considerations for safe electrical-stimulation of nervous-system with platinum-electrodes *IEEE Trans. Biomed. Eng.* **24** 59–63
- Cogan S F 2008 Neural stimulation and recording electrodes *Annu. Rev. Biomed. Eng.* **10** 275–309
- Cogan S F, Troyk P R, Ehrlich J and Plante T D 2005 *In vitro* comparison of the charge-injection limits of activated iridium oxide (AIROF) and platinum-iridium microelectrodes *IEEE Trans. Biomed. Eng.* **52** 1612–4
- Eversmann B *et al* 2003 A 128×128 CMOS biosensor array for extracellular recording of neural activity *IEEE J. Solid-State Circuits* **38** 2306–17
- Frey U, Egert U, Heer F, Hafizovic S and Hierlemann A 2009 Microelectronic system for high-resolution mapping of extracellular electric fields applied to brain slices *Biosens. Bioelectron.* **24** 2191–8
- Hai A, Shappir J and Spira M E 2010 In-cell recordings by extracellular microelectrodes *Nat. Methods* **7** 200–U50
- Hambrecht F T 1979 Neural prostheses *Annu. Rev. Biophys. Bioeng.* **8** 239–67
- Heer F, Hafizovic S, Ugniwenko T, Frey U, Franks W, Perriard E, Perriard J C, Blau A, Ziegler C and Hierlemann A 2007 Single-chip microelectronic system to interface with living cells *Biosens. Bioelectron.* **22** 2546–53
- Holmgren C, Harkany T, Svennenfors B and Zilberter Y 2003 Pyramidal cell communication within local networks in layer 2/3 of rat neocortex *J. Physiol.* **551** 139–53
- Hutzler M, Lambacher A, Eversmann B, Jenkner M, Thewes R and Fromherz P 2006 High-resolution multitransistor array recording of electrical field potentials in cultured brain slices *J. Neurophysiol.* **96** 1638–45
- Lambacher A, Jenkner M, Merz M, Eversmann B, Kaul R A, Hofmann F, Thewes R and Fromherz P 2004 Electrical imaging of neuronal activity by multi-transistor-array (MTA) recording at 7.8 μm resolution *Appl. Phys. A* **79** 1607–11
- Lei N, Watson B O, MacLean J N, Yuste R and Shepard K 2008 A 256×256 CMOS microelectrode array for extracellular neural stimulation of acute brain slices *Int. Solid-State Circuit Conf.* vol 51 pp 147–8
- Lutz C, Otis T S, DeSars V, Charpak S, DiGregorio D A and Emiliani V 2008 Holographic photolysis of caged neurotransmitters *Nat. Methods* **5** 821–7
- Matsuzaki M, Ellis-Davies G C and Kasai H 2008 Three-dimensional mapping of unitary synaptic connections by two-photon macro photolysis of caged glutamate *J. Neurophysiol.* **99** 1535–44
- Nikolenko V, Poskanzer K E and Yuste R 2007 Two-photon photostimulation and imaging of neural circuits *Nat. Methods* **4** 943–50
- Potter S M and DeMarse T B 2001 A new approach to neural cell culture for long-term studies *J. Neurosci. Methods* **110** 17–24
- Rose T L, Kelliher E M and Robblee L S 1985 Assessment of capacitor electrodes for intracortical neural stimulation *J. Neurosci. Methods* **12** 181–93
- Rose T L and Robblee L S 1990 Electrical stimulation with Pt electrodes: VIII. Electrochemically safe charge injection limits with 0.2 ms pulses *IEEE Trans. Biomed. Eng.* **37** 1118–20
- Schoen I and Fromherz P 2007 The mechanism of extracellular stimulation of nerve cells on an electrolyte-oxide-semiconductor capacitor *Biophys. J.* **92** 1096–111
- Stensaas S S and Stensaas L J 1978 Histopathological evaluation of materials implanted in the cerebral cortex *Acta Neuropathol.* **41** 145–55
- Thiebaud P, deRooij N F, Koudelka-Hep M and Stoppini L 1997 Microelectrode arrays for electrophysiological monitoring of hippocampal organotypic slice cultures *IEEE Trans. Biomed. Eng.* **44** 1159–63
- Thomson A M, West D C, Wang Y and Bannister A P 2002 Synaptic connections and small circuits involving excitatory and inhibitory neurons in layers 2–5 of adult rat and cat neocortex: triple intracellular recordings and biocytin labelling *in vitro Cereb. Cortex* **12** 936–53
- Wang H *et al* 2007 High-speed mapping of synaptic connectivity using photostimulation in channel rhodopsin-2 transgenic mice *Proc. Natl Acad. Sci. USA* **104** 8143–8